Anti-symmetric Fourier Descriptor for Non-closed Segments

Jian-Jiun Ding, *Member, IEEE,* Wei-Lun Chao, *Student Member, IEEE,* Jiun-De Huang, and Cheng-Jin Kuo

***Abstract*—The Fourier descriptor is an efficient and effective way to record and compress a closed boundary: A few low-frequency coefficients are sufficient to reconstruct the contour of the original boundary. However, for a non-closed segment, since the two non-adjacent end points result in signal discontinuity, the reconstructed segment after eliminating the high-frequency part has significant distortion around the two ends. In this paper, we propose a new Fourier descriptor scheme to deal with this problem. The proposed scheme first warps the non-closed segment into a closed one, performs *anti-symmetric extension* around the two end points to smooth the warped segment, and finally adopts the conventional Fourier descriptor for segment recording. Based on this scheme, the high-frequency components near the two ends are much reduced, and a more accurate reconstructed segment with the exact end-point locations can be achieved. Furthermore, the proposed scheme could also be applied on closed boundaries with a pre-segmentation process: segmenting the closed boundary at sharp corners and generating several smooth non-closed segments. According to the simulation results under the same compression rates, the proposed method has better reconstruction quality than directly extracting the Fourier descriptor on closed boundaries.**

***Index Terms*—Fourier descriptor; data compression; discrete Fourier transforms; image coding; shape description**

I. Introduction

IN image processing and pattern recognition, boundary (or edge) description plays an important role not only for shape feature extraction, but also for efficient contour recording and reconstruction. Among existing boundary description methods, the Fourier descriptor is widely used because of its rotation, scaling, and translation invariant (RST-invariant) properties and its *compressibility*: A few coefficients, generally the low-frequency ones, are sufficient to describe and reconstruct the closed shape boundary approximately [3], [15]. However, when dealing with a non-closed segment, the compressibility may severely degrade due to the two non-adjacent end points, which form signal discontinuity and lead to significant high-frequency coefficients. That is, if these high-frequency coefficients are directly removed for boundary compression, the reconstructed segment will tend to be closed, resulting in strong distortions around the two ends. Fig. 1 illustrates this problem.

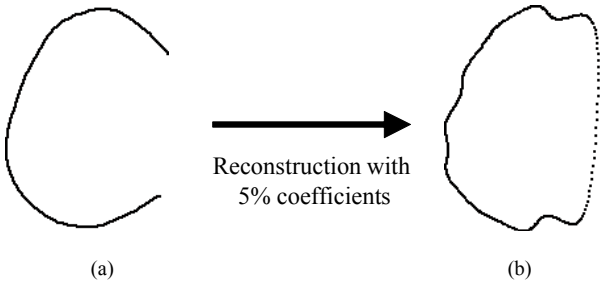

Fig. 1. The problem of using the conventional Fourier descriptor to compress and reconstruct the non-closed segment: (a) the original segment; (b) the reconstruction segment with 5% Fourier coefficients at the low-frequency part. As shown, truncation the high-frequency coefficients results in severe distortion around the two end points.

To solve the above problem for non-closed segments, in this paper we propose a new Fourier descriptor scheme, which introduces two preprocessing steps — *linear offset* and *anti-symmetric extension* — before extracting the conventional Fourier descriptor [3]-[4], [15]. The first step, *linear offset*, warps the non-closed segment into a closed contour; the second step, *anti-symmetric extension*, then smoothes the warped segment by making the first-order differences at the end points continuous. These two steps jointly reduce the high-frequency coefficients in the original non-closed segment, especially the ones caused by the two ends; the resulting closed segment could be approximately reconstructed by only a few low-frequency coefficients. Later by performing the inverse operations of the two preprocessing steps on the reconstructed closed segment, a more accurate non-closed segment then can be rebuilt without degrading the compressibility. Furthermore, the end point locations of the original segment are perfectly preserved in the reconstructed segment under any compression rate.

The proposed Fourier descriptor scheme could also be applied on closed boundaries to achieve better reconstruction quality. In the general usage of Fourier descriptors, the discrete Fourier transform (DFT) is directly performed on the whole boundary sequence, whereas under high compression rates, details such as corners and sharp angles will be destroyed. In our method, a closed boundary is first divided into several non-closed yet smooth segments according to its corners and sharp angles. The proposed Fourier descriptor scheme is then applied to record these non-closed segments. Simulation results show that under the same compression rates, our method could preserve more detail structures than the general method on closed boundaries.

Manuscript received Sept. 2012. This work was supported by the National Science Council, R.O.C., under the contract 101-2221-E-002-020.

The authors are with the Graduate Institute of Communication Engineering, National Taiwan University, Taipei, Taiwan, 10617, R.O.C. (e-mail: djj@cc.ee.ntu.edu.tw, weilunchao760414@gmail.com, knuckles3289@yahoo.com.tw, r96921039@ntu.edu.tw)

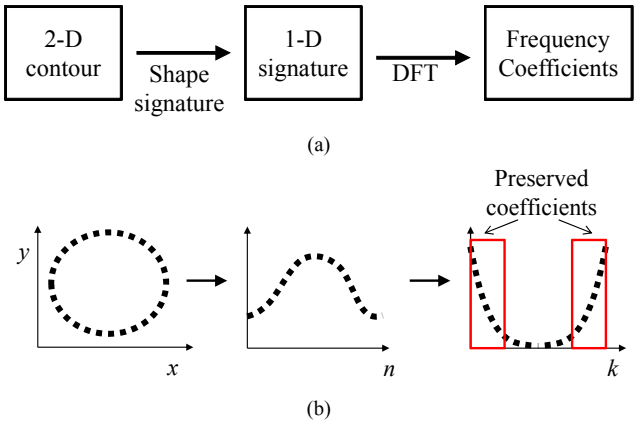

Fig. 2. The general procedure of Fourier descriptors: (a) the flowchart with 2 stages: shape signature and the DFT; (b) an example to illustrate the input and output of the two stages. For efficient recording and description, only the low-frequency coefficients are preserved.

The contributions of this paper are summarized as follows:

- A new Fourier descriptor scheme is presented to compress and reconstruct the non-closed segments, which maintains the compressibility and exactly preserves the end point locations.
- The proposed Fourier descriptor scheme could also be used on closed boundaries with a pre-segmentation process. This method outperforms the general method under the same compression rates for boundary reconstruction.
- Extensive simulations on several Chinese characters and the standard MPEG-7 CE-shape-1 database [8] are conducted.

This paper is organized as follows: In Section II, we briefly review the concept of Fourier descriptors and previous work on non-closed segments. In Section III, the proposed Fourier descriptor scheme for non-closed segments is presented. The extension of the proposed scheme towards closed boundaries is described in Section IV. In Section V, several simulations are performed to demonstrate the effectiveness of our method on both closed and non-closed contours. Finally, in Section VI, we conclude this paper.

II. Review of Fourier Descriptors

A. The Basic Concept of Fourier Descriptors

According to existing literatures, Fourier descriptors have two main purposes in practice: One is to extract a compact shape descriptor for matching and retrieval [2], [4]-[5], [7]-[8], [10], [13]-[14], [18]; the other is to efficiently record and compress the boundaries [4][11][16][19], which is *the major concern of this paper*.

The Fourier descriptor algorithm consists of two stages: *shape signature* and *discrete Fourier transform* (DFT). The first stage maps the 2-D boundary into a 1-D sequence, called the shape signature [18]; the second stage then applies the DFT on this 1-D signature, resulting in a set of DFT frequency coefficients to represent the boundary. To describe and record the boundary efficiently, only the low-frequency coefficients are kept. Fig. 2 shows the procedure of Fourier descriptors.

In general, the second stage is seen as a fixed operation, so previous work of Fourier descriptors primarily focuses on how to design the shape signatures process. For example, Zahn *et al.* [19] proposed the cumulative angular function along the boundary; Granlund [4] used the complex coordinate, denoted as the *conventional Fourier descriptor* in this paper. In [20][21] Zhang *et al.* gave comparative studies among several existing shape signatures on the matching performance. An important characteristic of shape signatures is the *reversibility*: If the shape signature is not reversible from the 1-D sequence to the 2-D boundary, it is not available for boundary reconstruction.

There is also some work aiming to explore the RST-invariant properties and to design the matching metric for accurate image retrieval [1], [13]. And in [22], Zhang *et al.* presented a special Fourier descriptor algorithm that performs the 2-D Fourier transform on the whole image rather than performs the 1-D Fourier transform on the boundary sequence.

B. Fourier Descriptors for Non-closed Segments

The Fourier descriptors mentioned above are mainly used for closed boundaries. However, for non-closed segments, which frequently occur in character recognition and edge recording, their performances may degrade due to the non-adjacent end points. That is, the non-adjacent end points lead to signal discontinuity at the two ends of the 1-D signature, resulting in significant high-frequency coefficients that cannot be directly eliminated for contour recording.

To solve this problem, the shape signature process should be designed to produce a signature with similar end point values. In previous work, Uesaka [16] computed the sequential point difference along a contour as the shape signature. His method does reduce the high-frequency components in the shape signature and preserve the exact end point locations, but the equal-length sampling process is not suitable for digital images. In [11], Nijim first extended the non-closed segment at the two ends, and then applied the Fourier descriptor. He claimed that after compression, the distortion would only appear at the extended part, and the original end points could be preserved; the extended length, however, is remained undefined. In [17], Weyland *et al.* proposed the generalized Fourier descriptor by modifying the cumulative angular function, whereas it has been mentioned in [16], [21] that this function has slow convergence speed and is not suitable for boundary compression.

Another method to solve the non-closed segment problem is to perform the discrete cosine transform (DCT) rather than the DFT on the shape signature. Namely, the shape signature is first extended into the even-symmetric form, which indeed has same end point values; the DFT is then applied to get the frequency coefficients for contour recording. Although this method is efficient and could alleviate the distortions after compression, the end point locations are not guaranteed to be preserved.

III. The Proposed Fourier Descriptor Scheme

In this paper, our main concerns are boundary compression and reconstruction rather than the matching and retrieval

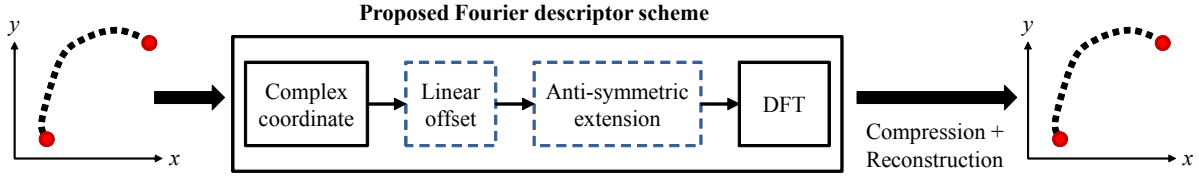

Fig. 3. The flowchart of the proposed Fourier descriptor scheme. Given a non-closed segment, the complex-coordinate mapping first records the segment as a 1-D complex sequence. Then, the proposed ***linear-offset*** and ***anti-symmetric extension*** (illustrated by the blue dash boxes) are performed to close and smooth the segment. Finally, the DFT is executed to achieve the frequency coefficients for boundary compression. The main goal of our scheme is to approximately reconstruct the non-closed segment with the exact endpoint locations.

purposes, meaning that the shape signature process should be reversible. Instead of designing a new reversible shape signature with similar end point values for non-closed segments, we adopt the complex-coordinate mapping [4] (a reversible signature) and present two modification steps — *linear offset* and *anti-symmetric extension* — to close and smooth the original non-closed segment. With these modifications, the final 1-D sequence fed into the DFT would have much smaller high- frequency components (as in Fig. 5) and could be approximately reconstructed by the low-frequency coefficients. In addition, no matter how many DFT coefficients are remained for boundary compression, our scheme is proved to keep the *exact end point locations* after reconstruction. Fig. 3 depicts the flowchart of the proposed Fourier descriptor scheme, and in the following sub- sections, we describe each step in order. Note that the complex- coordinate step could be placed after anti-symmetric extension without causing any difference to the resulting descriptor.

A. The Complex-coordinate Mapping

Given an N-point boundary $\{(x_n, y_n) | n = 0,1,.....,N-1\}$, the complex-coordinate mapping [4] represents each contour point as a complex number and generates a complex sequence $s(n)$ as follows:

$$s(n) = x(n) + jy(n), \text{ for } k = 0,1,.....,N-1 \quad (1)$$

where the x-axis is treated as the real part; the y-axis, imaginary part. If the boundary is not closed, the sequence $s(n)$ is obviously discontinuous at the two ends and its DFT will contain large high-frequency coefficients.

B. Linear Offset

To reduce the high-frequency components derived from the non-adjacent end points, an intuitive idea is to warp the original segment into a closed one. In this paper, we present a linear offset algorithm to achieve this goal: A contour point (x_n, y_n) on the original segment is linearly shifted to (x_n', y_n') based on the following rule:

$$\begin{aligned} x_n' &= x_n - x_0 - \{(x_{N-1} - x_0) \times n/(N-1)\}, \\ y_n' &= y_n - y_0 - \{(y_{N-1} - y_0) \times n/(N-1)\}, \\ &\text{for } n = 0,1,.....,N-1. \end{aligned} \quad (2)$$

Note that $x_0' = x_{N-1}' = 0$ and $y_0' = y_{N-1}' = 0$. This rule shifts each contour point according to its index and the difference between the end points. The warped segment then becomes a closed one

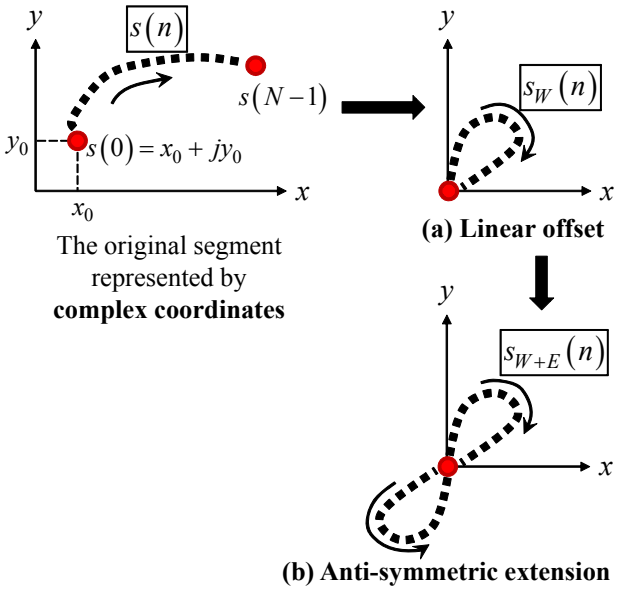

Fig. 4. The illustration of performing (a) ***linear-offset*** (resulting in a sharp angle at the origin) and (b) ***anti-symmetric extension*** on a non-closed segment. As shown, the output segment after these two steps become a closed one and has continuous first-order differences at the two end points.

named $s_W(n)$, which is shown as in Fig. 4(a):

$$s_W(n) = \{(x_n', y_n') | n = 0,1,.....,N-1\}. \quad (3)$$

The linear offset algorithm is reversible from (x_n', y_n') back to (x_n, y_n) by keeping the two end point locations, ensuring its availability for boundary reconstruction. And as illustrated in Fig.5, *the resulting closed segment has smaller high-frequency components than the original non-closed one*; the reconstructed segment from $s_W(n)$ with 2.5% compression rate could preserve the non-closed shape. The compression rate and reconstruction process are described later in Sections III-D and III-E.

However, even after linear offset, the linked two ends may lead to a sharp angle on the contour, therefore still containing high-frequency components. In addition, the end point locations are not guaranteed to be preserved after reconstruction.

C. Anti-symmetric Extension

To smooth the sharp angle generated by the linear offset, we further propose the anti-symmetric extension scheme by adding

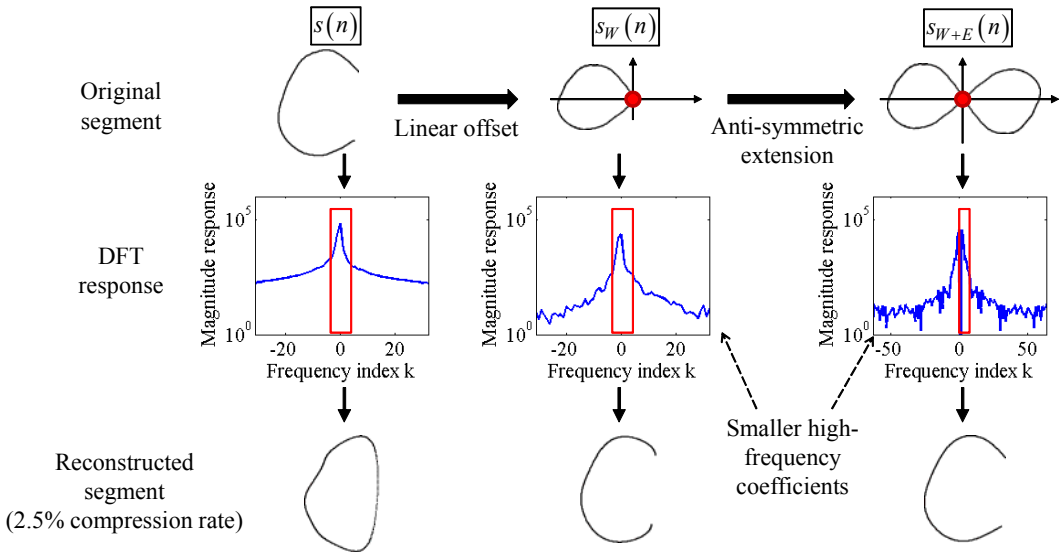

Fig. 5. Illustrations of the ***segment shapes*** (Row 1), ***DFT responses*** (Row 2), and ***reconstruction shapes*** with 2.5% coefficients (Row 3) after applying linear offset (Column 2) and anti-symmetric extension (Column 3). The original segment is 321-point long and its DFT has 321 coefficients. The anti-symmetric extended segment is 640-point long then with 640 coefficients; however, only part of them are essential. For clearness, in Row 2 only 20% of the coefficients around the zero frequency are shown; ***the magnitude responses are plotted in the log scale***. Row 3 shows the reconstructed segments with only 8 complex values (about 2.5% of the original 321 coefficients) based on each input signatures. The red boxes in Row 2 mark the coefficients preserved, and for $s_W(n)$ and $s_{W+E}(n)$, 2 of the 8 remained complex values are the end point locations.

an anti-symmetric segment of $s_W(n)$ behind $s_W(n)$, as illustrated in Fig. 4(b). The new (2N-2)-point segment $\boldsymbol{s_{W+E}(n)}$, with **W**arping and **E**xtension, is defined as follows:

$$s_{W+E}(n)=\begin{cases} s_W(n) & \text{, for } n=0,1,...,N-1 \\ -s_W(2N-2-n) & \text{, for } n=N,...,2N-3 \end{cases}, \quad (4)$$

which is closed and has continuous first-order and zero second-order differences at the two end points (hence much smoother). Note that adding the anti-symmetric segment in $s_{W+E}(n)$ does not increase the amount of coefficients to preserve, since the DFT frequency response of an anti-symmetric signal is also anti- symmetric. Therefore, only half of the Fourier coefficients of $s_{W+E}(n)$ are required to keep for lossless reconstruction.

As illustrated in Fig. 5, *$s_{W+E}(n)$ has even smaller high-frequency components than $s_W(n)$*; besides, the reconstructed segment from $s_{W+E}(n)$ with 2.5% compression rate has better quality — with *the exact end point locations* — than that from $s(n)$ and $s_W(n)$.

D. DFT and Boundary Compression

After linear offset and anti-symmetric extension, the resulting sequence $s_{W+E}(n)$ is then fed into the DFT to get the frequency coefficients $S(k)$:

$$S(k)=\frac{1}{2N-2}\sum_{k=0}^{2N-3} s_{W+E}(k)e^{-j2\pi nk/(2N-2)}. \quad (5)$$

Since $s_{W+E}(n)$ is of zero mean and $S(k)$ is anti-symmetric with $S(k) = -S(2N\text{-}2\text{-}k)$, both $S(0)$ and $S(N\text{-}1)$ are 0. Thus to achieve lossless reconstruction, only $S(k)$ at k = 1, 2, ……, N-2 are required.

For boundary compression, the first P coefficients ($S(k)$ at k = 1, 2, ……, P; $0 \leqq P \leqq N$-2) are remained, and totally P+2 complex values, including the two end point locations, are recorded for reconstruction. The compression rate (CR) utilized in this paper is defined as:

$$CR=\frac{\#\text{ recorded complex values}}{\#\text{ original segment length}}\times 100\%. \quad (6)$$

For the proposed scheme, CR is computed as:

$$CR=\frac{P+2}{N}\times 100\%. \quad (7)$$

E. Boundary Reconstruction from the Proposed Scheme

The reconstruction process from the preserved P coefficients and the two end point locations is listed as follows:

- **(Step1):** Regenerate the (2N-2)-long frequency response $S^*(k)$ from the P preserved coefficients by zero padding and anti-symmetric extension.
- **(Step 2):** Perform the inverse DFT to get $s_{W+E}{}^*(n)$.
- **(Step 3):** Eliminate the anti-symmetric part in $s_{W+E}{}^*(n)$ to get $s_W{}^*(n)$ and perform the inverse operations of (2) to achieve the reconstructed segment $s^*(n)$.

In Fig. 6, both the boundary compression and reconstruction processes are summarized.

F. Proof of the Exact End Point Preserving Property

In this subsection, we give the proof of the exact end point

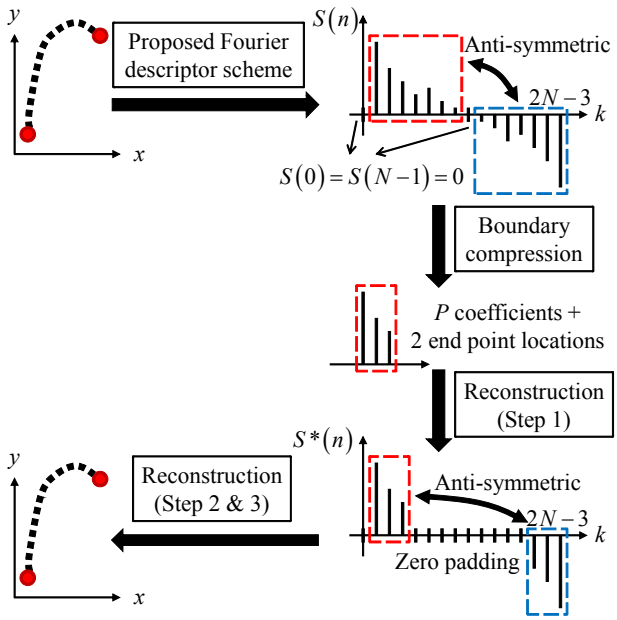

Fig. 6. Illustrations of both the boundary compression and the reconstruction processes: After applying the proposed scheme, P of the coefficients and the two end point locations are remained for boundary recording. To reconstruct the non-closed segment, we first regenerate the (2N-2)-long coefficient sequence (Step 1) and then perform Steps 2 & 3 in Section III-D to achieve it.

preserving property of the proposed Fourier descriptor scheme: No matter how many DFT coefficients are remained, the end points of the reconstructed segment will coincide with those of the original segment. This proof can be achieved by checking $s_W^*(0)$ and $s_W^*(N\text{-}1)$, which are the end point locations of the reconstructed segment of $s_W(n)$. As mentioned in (2), the two end values of $s_W(n)$ are 0; then if $s_W^*(0)$ and $s_W^*(N\text{-}1)$ are also 0, the reconstructed non-closed segment $s^*(n)$ after the inverse operations of (2) will have the same end points as what $s(n)$ has. The formulas of $s_W^*(0)$ and $s_W^*(N\text{-}1)$ are presented as follows:

$$\begin{aligned} s_W^*(0) &= \sum_{k=1}^{P} S(k)\, e^{j2\pi 0k/(2N-2)} + \sum_{k=2N-2-P}^{2N-3} S(k)\, e^{j2\pi 0k/(2N-2)} \\ &= \sum_{k=1}^{P} S(k) + \sum_{k=2N-2-P}^{2N-3} S(k) \\ &= \sum_{k=1}^{P} [S(k) + S(2N-2-k)] = 0, \end{aligned} \tag{8}$$

$$\begin{aligned} s_W^*(N-1) &= \sum_{k=1}^{P} S(k) e^{j2\pi(N-1)k/(2N-2)} + \sum_{k=2N-2-P}^{2N-3} S(k) e^{j2\pi(N-1)k/(2N-2)} \\ &= \sum_{k=1}^{P} S(k) e^{j\pi k} + \sum_{k=2N-2-P}^{2N-3} S(k) e^{j\pi k} \\ &= \sum_{k=1}^{P} [S(k) + S(2N-2-k)] e^{j\pi k} = 0 \end{aligned} \tag{9}$$

where the anti-symmetric property of S(k) is considered, which is derived from the proposed anti-symmetric extension; without anti-symmetric extension, the end point preserving property is not guaranteed after boundary compression. Note that both (8) and (9) are held under arbitrary P ($0 \leqq P \leqq N\text{-}2$).

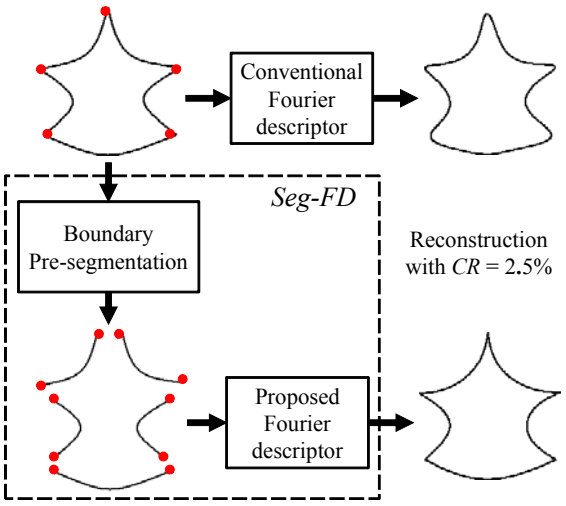

Fig. 7. The flowchart and illustration of the proposed *Seg-FD* framework for closed boundary: The top row shows the reconstruction result using the conventional Fourier descriptor [4] with 2.5% compression rate. The bottom part shows the result of *Seg-FD* (the dash box). As shown, the proposed *Seg-FD* framework could lead to better reconstruction quality, ***especially around the corners***.

IV. The Proposed Method for Closed Boundaries

The proposed Fourier descriptor scheme could directly be applied on closed boundaries; the resulting Fourier descriptors and reconstructed boundaries are similar to the ones achieved by applying the convectional Fourier descriptor [3]-[4], [15] — since the linear offset step mentioned in Section III-B does not change the shapes of the originally closed boundaries.

Generally, Fourier descriptors are very efficient and effective for recording closed boundaries; under high compression rates, however, detailed structures of the original boundaries such as corners and sharp angles still cannot be maintained. To alleviate this problem, we further propose a framework named ***Seg-FD***:

Seg-FD performs boundary ***S***egmentation at first to generate several non-closed yet smooth segments, and then applies the proposed ***F***ourier ***D***escriptor scheme to record these segments. The flowchart of *Seg-FD* is depicted in Fig. 7.

A. Boundary Pre-segmentation

In order to create smooth non-closed segments, sharp angles or corners on the closed boundary should be detected first; the closed boundary is then divided at these positions into several non-closed segments containing no corners inside. There have been many corner detection algorithms in existing literatures, like the Harris corner detector [6], SIFT [9], and the machine learning approach in [12]. These methods, nevertheless, are designed mainly for corner detection in regular images, and either with high computational complexity or requiring a learning step. For our cases on binary contour images and for efficient detection, a simple algorithm through checking the inner products along contours (shown in Fig. 8) is utilized.

Given an N-point boundary $\{(x_n, y_n) | \, n = 0, 1, \ldots, N\text{–}1\}$this corner detection algorithm goes through each point (x_n, y_n) in

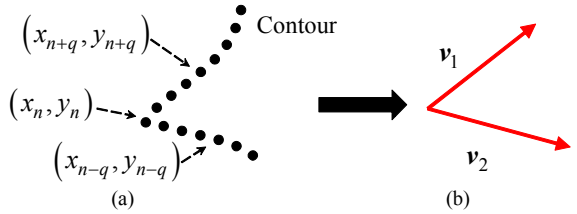

Fig. 8. The corner detection algorithm used in our paper: (a) for each point on the contour, two neighboring points (with $q = 4$) are selected; (b) The two vectors generated by (10) are used to compute the normalized inner product.

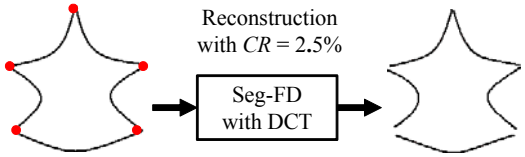

Fig. 9. The illustration of applying the complex coordinates [4] (for shape signatures) and the DCT in *Seg-FD*: The compression rate is 2.5%. Without the end point preserving property, the reconstructed segment is broken at the corners.

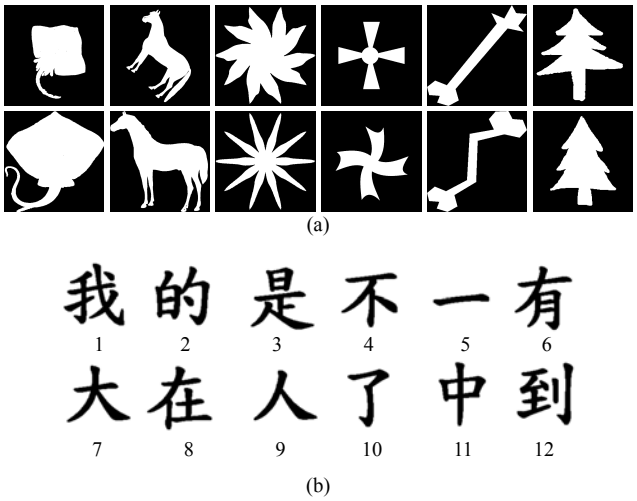

Fig. 10. Samples of the two data sets used in our simulations: (a) the MPEG -7 Core Experiment CE-shape-1 Part B database (each column shows two samples of the same class); (b) the Chinese character data set collected by ourselves (the number below each sample shows its frequency rank).

turn and computes the normalized inner product $NIP(n)$ defined as follows:

$$NIP(n) = \frac{\boldsymbol{v}_1 \bullet \boldsymbol{v}_2}{\|\boldsymbol{v}_1\|\|\boldsymbol{v}_2\|},$$
$$\text{with } \boldsymbol{v}_1 = \left[x_{n+q} - x_n,\ y_{n+q} - y_n\right]^T, \quad (10)$$
$$\boldsymbol{v}_2 = \left[x_{n-q} - x_n,\ y_{n-q} - y_n\right]^T$$

where q is an index offset (e.g. $q = 4$) for defining $\boldsymbol{v}_1$ and $\boldsymbol{v}_2$. If $NIP(n)$ is larger than a predefined threshold, (x_n, y_n) is marked as a corner on the contour; the detected corners are then sorted according to their *NIP*s in the descending order, and the top L corners are selected for boundary segmentation. To prevent too close corners, a lower bound of corner intervals is also defined.

B. Boundary Compression

After segmenting the closed boundary into L non-closed segments, the proposed Fourier descriptor scheme is applied on these segments: each segment is recorded by a number of coefficients proportional to its length. Although one segment has two end points, the total number of end points to keep is just L since two segments share a common end point (corner).

For boundary compression at $CR = K/N \times 100\%$, the total number of recorded DFT coefficients P and corners L are summed to be K, leading to a balancing problem on P and L. In our implementation, a balance parameter BP ($0 \leqq BP \leqq 1$) is set to restrict the number of corners; that is, $L \leqq BP \times K$, meaning that at most $\lfloor BP \times K \rfloor$ corners are selected (based on their *NIP* values) for boundary segmentation.

C. Boundary Reconstruction

Boundary reconstruction is achieved by first rebuilding the L non-closed segments and then linking them together. Thanks to the *end point preserving property*, the reconstructed non-closed segments exactly keep the end point locations, guaranteeing that the reconstructed whole boundary is continuous, with no rifts at the corners. Except for the proposed Fourier descriptor scheme and Uesaka's method [16], *other Fourier descriptors do not have this property and cannot be applied in the Seg-FD framework for non-closed segment recording.* Fig. 9 shows the case of using the DCT (with the complex-coordinate mapping) in *Seg-FD*: The reconstruct boundary is broken at the corners.

V. Simulation Results

In this section, several experiments of boundary compression (reconstruction) are conducted to demonstrate the effectiveness of the proposed methods. For non-closed segments, we compare the proposed Fourier descriptor with the conventional Fourier descriptor [4], Uesaka's method [16], Nijim's method [11], and the DCT method that uses the complex coordinate as the shape signature; other shape signatures introduced in Section II-A or surveyed in [20], [21] are not included because they are not reversible. And for closed boundaries, our *Seg-FD* framework is compared with the conventional Fourier descriptor [4].

A. Data Sets and Evaluation Criteria

Two data sets are utilized in the experiments: One is the MPEG-7 Core Experiment CE-shape-1 Part B [8] (MPEG-7 database in short), which contains 1400 shape contour images from 70 object classes, each class with 20 images; the other is a Chinese character data set with the most frequently-used 50 characters, collected by ourselves. Fig. 10 shows some samples of these two data sets. Note that in the MPEG-7 database, each image may contain more than one closed contours, and only the largest one is selected to represent each image.

To evaluate the reconstruction performance, the normalized $L1$ and $L2$ distances (normalized by the contour length) between the original contour $s(n)$ and reconstructed contours $s^*(n)$ are computed as the reconstruction errors:

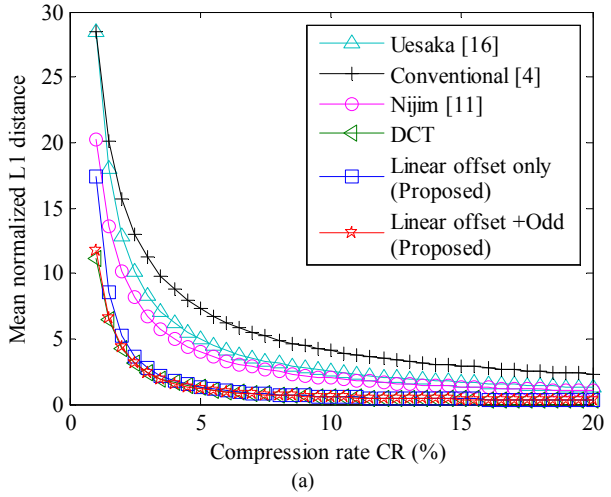

(a)

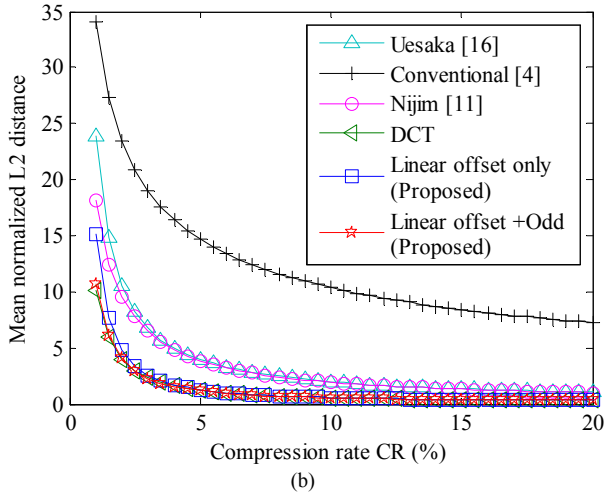

(b)

Fig. 11. The average ***reconstruction errors*** of non-closed segments computed on the MPEG-7 database under varied compression rates: (a) the average normalized $L1$ error; (b) the average normalized $L2$ error. The proposed methods (linear offset + odd extension) and the DCT methods have the least reconstruction errors.

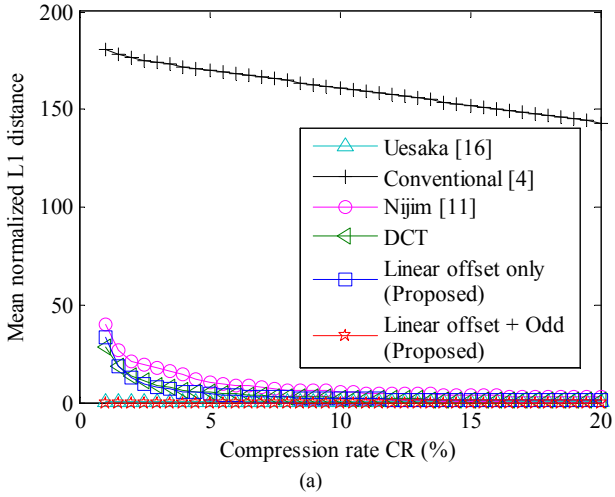

(a)

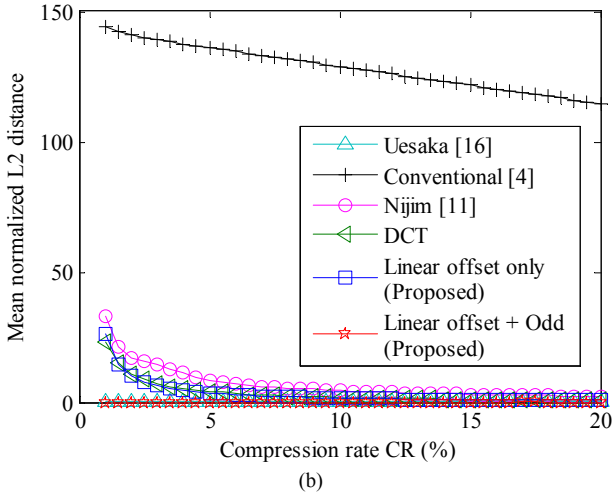

(b)

Fig. 12. The average ***end point errors*** of non-closed segments computed on the MPEG-7 database under varied compression rates: (a) the average normalized $L1$ error (normalized by 2); (b) the average normalized $L2$ error. The proposed methods (linear offset + odd extension) also have the least end point error, but the DCT method has large end point error.

$$n\_L1 = \sum_{n=1}^{N} \left\{ \left| real\left(s(n) - s^*(n)\right) \right| + \left| imag\left(s(n) - s^*(n)\right) \right| \right\} / N, \quad (11)$$

$$n\_L2 = \left(\sum_{n=1}^{N} \left| s(n) - s^*(n) \right|^2 / N \right)^{1/2} \quad (12)$$

where N means the contour length. Note that by using Fourier descriptors for boundary compression, the reconstructed contour always has the same length as the original contour.

B. Simulations on Non-closed Segments

On boundary compression and reconstruction of non-closed segments, the proposed Fourier descriptor is compared with methods in [4], [11], [16], and the DCT method. As mentioned in Section II-B, Uesaka's method [16] was not designed for digital images originally. To enable its usage in our simulations, we modified the shape signature in [16] as the following form:

$$s_{Uesaka}(n) = s(n+1) - s(n), \text{ for } n = 0, 1, ..., N-2 \quad (13)$$

where $s(n)$ is the complex-coordinate sequence defined in (1). The first point $s(0)$ in $s(n)$ should be recorded for reversibility (like the end point locations recorded in our scheme). And for Nijim's method [11], the extension length at each end is set as 0.07 of the original segment length.

The MPEG-7 database is utilized for simulations where part of each image contour (60% in our implementation) is extracted as the non-closed segment. To prevent that under extremely high compression rates (e.g. 1%) the proposed scheme may not have enough space to record the two end points, only the larger 1299 segments (832.2 contour points in average) are involved for evaluation. The average reconstruction errors of different Fourier descriptors under varied compression rates (from 1% to 20%) are shown in Fig. 11 where the compression rate is defined in (6) and (7). As

Original	Conventional [4]	Uesaka's [16]	Nijim's [11]	DCT	**Proposed scheme**	*CR*
end point locations: **(1,357), (258,129)**	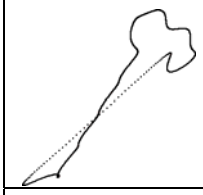	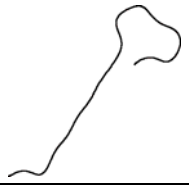	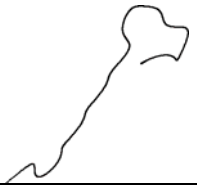	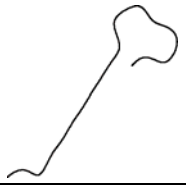	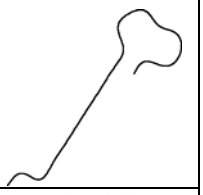	3%
	*L*1 = 15.01 end points: (131,238), (138,231)	*L*1 = 15.38 end points: (1,357), (258,129)	*L*1 = 7.68 end points: (-13,365), (272,134)	*L*1 = 2.76 end points: (7,349), (262,121)	***L*1 = 1.92** **end points:** **(1,357), (258,129)**	
	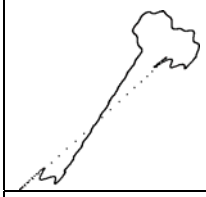	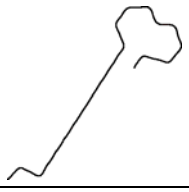	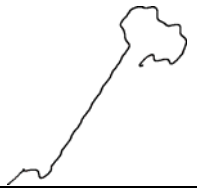	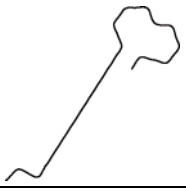	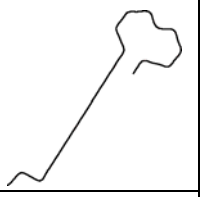	7%
	*L*1 = 7.55 end points: (122,249), (141,233)	*L*1 = 5.05 end points: (1,357), (258,129)	*L*1 = 3.37 end points: (-8,364), (267,121)	*L*1 = 0.64 end points: (3,355), (260,127)	***L*1 = 0.59** **end points:** **(1,357), (258,129)**	

(a)

Original	Conventional [4]	Uesaka's [16]	Nijim's [11]	DCT	**Proposed scheme**	*CR*
end point locations: **(2,88), (241,125)**						3%
	*L*1 = 15.90 end points: (125,95), (132,96)	*L*1 = 12.07 end points: (2,88), (241,125)	*L*1 = 8.12 end points: (-14,89), (256,133)	*L*1 = 3.02 end points: (5,79), (251,123)	***L*1 = 2.00** end points: **(2,88), (241,125)**	
	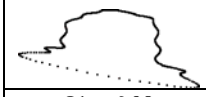					7%
	*L*1 = 6.98 end points: (114,104), (132,107)	*L*1 = 3.36 end points: (2,88), (241,125)	*L*1 = 3.83 end points: (8,88), (235,125)	*L*1 = 0.62 end points: (3,86), (243,125)	***L*1 = 0.53** **end points:** **(2,88), (241,125)**	

(b)

Fig. 13. Simulations of the reconstructed segments at *CR* = 3% and 7% where the ***normalized L1 reconstruction errors*** and the ***end point locations*** are also shown. The proposed Fourier descriptor scheme leads to the best reconstruction performance with exact end point location preservation.

presented, the proposed scheme with only the linear offset operation drastically lowers the reconstruction error of the conventional Fourier descriptor, and outperforms Nijim's and Uesaka's methods; the reconstruction performance could be further improved through anti-symmetric extension. The only algorithm that can compete with the proposed scheme is the DCT method.

To demonstrate the end point preserving property, we further compute the normalized end point error (normalized by 2) of each non-closed segment. The average errors are shown in Fig. 12 where only Uesaka's method and the proposed scheme (with both the two preprocessing steps) definitely preserve the end point locations. The DCT method, despite the comparable result with the proposed scheme in Fig. 10, could not preserve the end point location, especially under high compression rates. Based on the purpose of reducing the reconstruction and the end point error, the proposed scheme outperforms the compared methods.

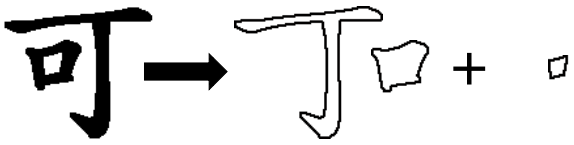

Fig.14. A Chinese character is separated into several outer or inner contours.

Fig. 13 presents several examples of reconstructed segments resulting from each method. As shown, the proposed scheme leads to the best reconstruction performance with exact end point preservation. Though Uesaka's method seems to produce plausible reconstructed shapes, its poor *L*1 errors disclose its drawback on compressing non-closed segments.

C. Simulations on Closed Boundaries

For the closed boundary case, we compare three methods — the conventional Fourier descriptor, *Seg-FD* + Uesaka's

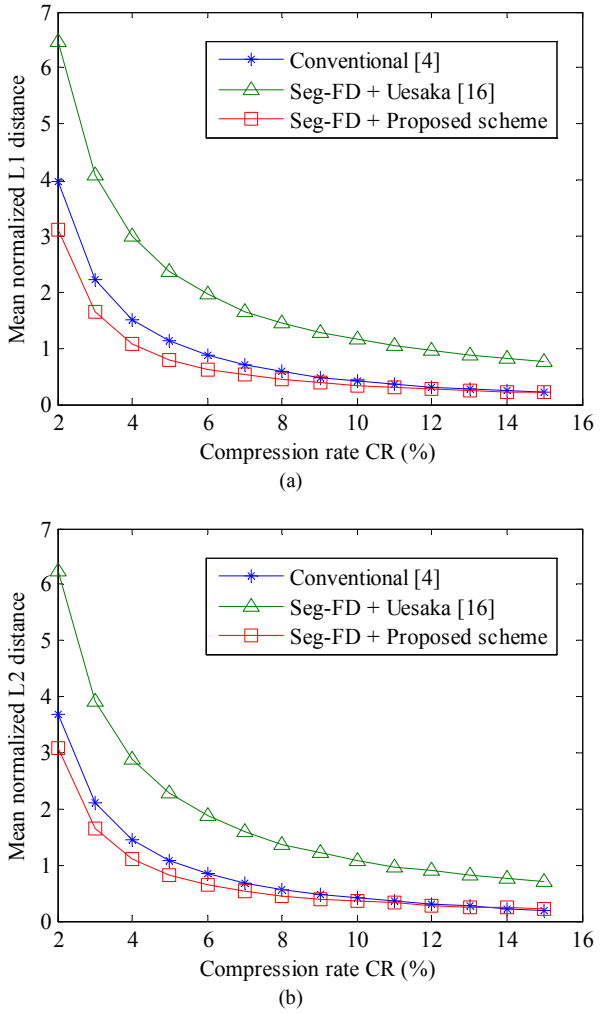

Fig. 15. The average ***reconstruction errors*** of closed boundaries computed on the MPEG-7 database under varied compression rates: (a) the average normalized $L1$ error; (b) the average normalized $L2$ error.

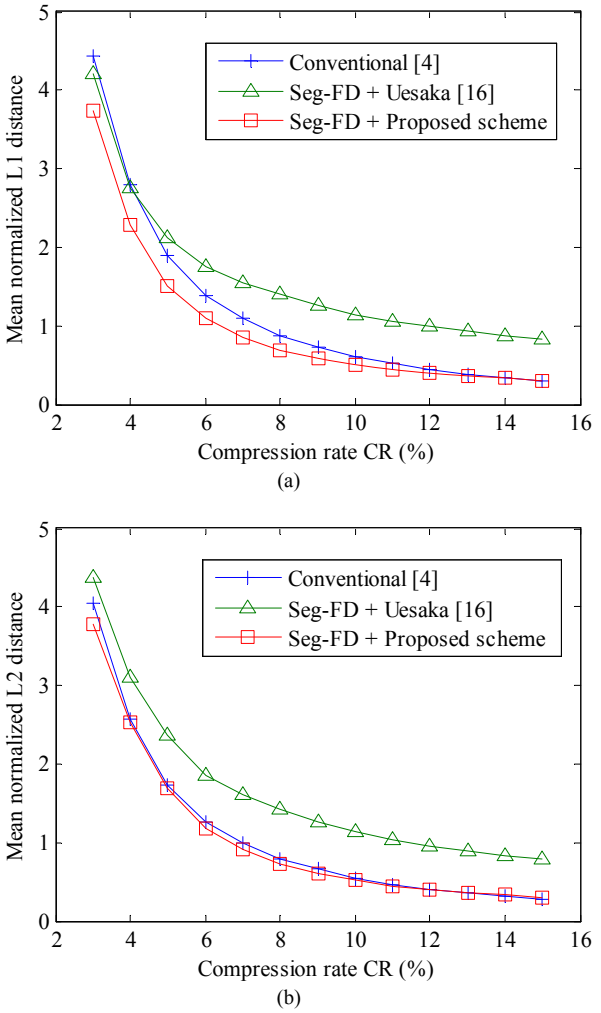

Fig. 16. The average ***reconstruction errors*** of closed boundaries computed on 50 Chinese characters under varied compression rates: (a) the average normalized $L1$ error; (b) the average normalized $L2$ error.

method, and *Seg-FD* + the proposed Fourier descriptor scheme — on both the MPEG-7 database and the 50 Chinese characters. Other Fourier descriptors included in the non-closed segment case are not considered in *Seg-FD* because of the lack of the end point preserving property. Since each Chinese character may contains several disconnected parts with outer or even inner contours (as illustrated in Fig. 14), *Seg-FD* and boundary compression are performed on each contour separately; the reconstruction error, nevertheless, is computed according to the whole character.'

As described in Section IV-B, a balance parameter BP is required to set in the proposed *Seg-FD* framework to allot the remained K complex values into P DFT coefficient and L corners ($P + K = L$). In our implementation, we go through 10 possible BPs (from 0.1 to 1 with a uniform 0.1 interval) and select the one that results in the lowest reconstruction error for each image. The case *Seg-FD* with $BP = 0$ is not considered since it is the conventional Fourier descriptor. The compression rate CR defined for *Seg-FD* is:

$$CR = \frac{K}{N} \times 100\% = \frac{P+L}{N} \times 100\%. \quad (14)$$

The average reconstruction errors computed on the MPEG-7 database (all the 1400 images are included) are shown in Fig. 15 where *Seg-FD* + the proposed scheme outperforms the other two methods, especially *Seg-FD* + Uesaka's method. This fact presents the advantage of applying the proposed scheme on recording non-closed segments against Uesaka's method. The experimental results also demonstrate the usage of *Seg-FD* (with the proposed Fourier descriptor scheme) for closed boundary compression. Fig. 18 presents several examples of the reconstructed closed boundaries at $CR = 0.3$ and 0.7.

In Fig. 16, the reconstruction errors computed on the 50 Chinese characters are present where *Seg-FD* + the proposed scheme still outperforms the other two methods, demonstrating its effectiveness on various shape types. Fig. 19 also presents

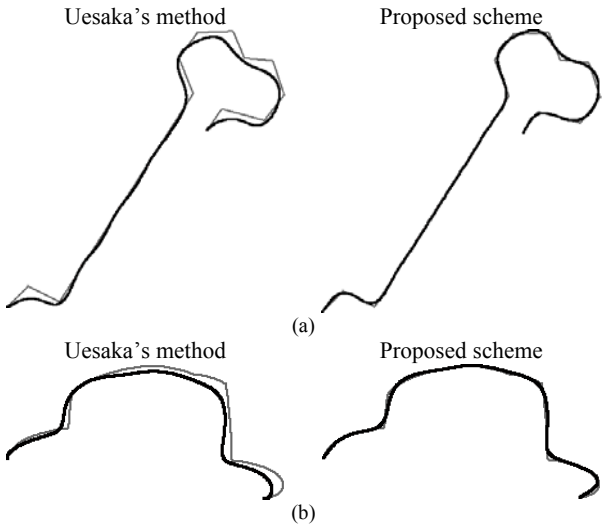

Fig. 17. The reconstruction results of Uesaka's method and the proposed scheme on the non-closed segments used in Fig. 13 at *CR* = 3%. The original segment is plotted in gray color. As presented, Uesaka's method has larger reconstruction error.

several reconstruction examples to illustrate the performance of *Seg-FD* on Chinese character compression. From the examples in Fig. 18 and Fig. 19, we found that when the original boundary is with many corners or sharp angles, the advantage of *Seg-FD* is much conspicuous. Even *Seg-FD* +Uesaka's method could result in a smaller reconstruction error than the conventional Fourier descriptor under this condition.

D. Discussions

Among the Fourier descriptor algorithms presented in this paper, only two of them could exactly preserve the end point locations of non-closed segments after boundary compression: One is the proposed scheme; the other is Uesaka's method [16]. When analyzing these two methods, we found a common trick used in the shape signature design — the subtraction operation. In (2), the proposed scheme subtracts a specific offset from each point based on the corresponding point index; the resulting closed segment, with the two ends located at the origin, enables the anti-symmetric extension and indirectly results in the end point preserving property. In (13), Uesaka's method computes the point difference along the contour as the signature, also leading to the end point preserving property as proved in [16].

From the experimental results, there is, however, an obvious performance gap between these two methods; that is, the reconstruction error of the proposed scheme is three to four times smaller than the one of Uesaka's method, though the reconstructed shape based on Uesaka's method looks plausible. To illustrate where the comparatively high error comes from, we plot each original segment used in Fig. 13 (in gray color) and the corresponding reconstructed result together inside one figure. As presented in Fig. 17, the reconstruction results of Uesaka's method clearly deviate from the original segments; on contrary, the results of the proposed scheme nearly overlap with the original segments.

This performance difference mainly results from the different usages of subtraction operations. In Uesaka's method, the reconstructed location of point n is based on the reconstructed location of n-1, according to (13). This process would lead to error propagation under high compression rates. The proposed scheme does not compute any subtraction between two points, except the point difference of the two ends, and therefore suffers no error propagation problem.

VI. Conclusion

This paper aims at high quality boundary compression on both non-closed segments and closed boundaries via the Fourier descriptor. To deal with the high-frequency coefficients caused by the non-adjacent end points of non-closed segments, a new Fourier descriptor scheme is proposed. The proposed scheme introduces two preprocessing steps — *linear offset* and *anti-symmetric extension* — to drastically reduce the high-frequency components around the two end points before applying the conventional Fourier descriptor. Based on this scheme, the compressibility of Fourier descriptors on closed boundaries can be maintained even on non-closed segments. Furthermore, the end point locations are exactly preserved after reconstruction under any compression rate. The proposed Fourier descriptor scheme could also be applied on closed boundaries by first segmenting a closed boundary into several non-closed yet smooth segments, which is called the *Seg-FD* framework in this paper.

According to the simulation results on the MPEG-7 shape database and several Chinese characters, the proposed Fourier descriptor scheme and the proposed *Seg-FD* framework do outperform other Fourier descriptor algorithms.

References

[1] I. Bartolini, P. Ciaccia, and M. Patella, "WARP: Accurate retrieval of shapes using phase of Fourier descriptors and time warping distance," *IEEE Trans. Pattern Analysis and Machine Intelligence*, vol. 27, no. 1, pp. 142-147, 2005.

[2] A. Folkers and H. Samet, "Content-based image retrieval using Fourier descriptors on a logo database," *Proc. ICPR*, pp. 521-524, 2002.

[3] R. C. Gonzalez and R. E. Woods, *Digital Image Processing*, 3rd Ed., Prentice Hall, New Jersey, pp. 815-822, 2008.

[4] G. H. Granlund, "Fourier preprocessing for hand print character recognition," *IEEE Trans. Computers*, vol. 21, iss. 2, pp. 195-201, 1972.

[5] P. R. G. Harding and T. J. Ellis, "Recognizing hand gesture using Fourier descriptors," *Proc. ICPR*, pp. 286-289, 2004.

[6] C. Harris and M. Stephens, "A combined corner and edge detector," *Proc. Alvey Vision Conference*, pp. 147-151, 1988.

[7] I. Kunttu and L. Lepisto, "Shape-based retrieval of industrial surface defects using angular radius Fourier descriptor," *IET Image Processing*, vol. 1, no. 2, pp. 231-236, 2007.

[8] L. J. Latecki, R. Lakamper, and U. Eckhardt, "Shape descriptors for non-rigid shapes with a single closed contour," *Proc. IEEE Conf. CVPR*, pp. 424-429, 2000.

[9] D. G. Lowe, "Distinctive image features from scale-invariant keypoints," *Int. Journal of Computer Vision*, vol. 60, no. 2, pp. 91-110, 2004.

[10] F. Marques, B. Llorens, and A. Gasull, "Prediction of image partitions using Fourier descriptors: application to segmentation-based coding schemes," *IEEE Trans. Image Processing*, vol. 7, iss. 4, pp. 529-542, 1998.

[11] A. Nijim, *Smart Dust: Distributed Behavior-Based Mobile Agents for Thinning Segmentation and Feature Extraction of Hand-Written Arabic and Chinese words*, M.S. thesis, Concordia University, Montreal, Quebec, Canada, 2004.

[12] E. Rosten and T. Drummond, "Machine learning for high-speed corner detection," *Proc. ECCV*, pp. 430-443, 2006.

[13] Y. Rui, A. C. She, and T. S. Huang, "Modified Fourier descriptors for shape representation — A practical approach," *Proc. Int. Workshop Image Databases and Multimedia Search*, 1996.

[14] V. Solachidis, N. Nikolaidis, and I. Pitas, "Watermarking polygonal lines using Fourier descriptors," *Proc. IEEE ICASSP*, pp. 1955-1958, 2000.

[15] S. Theodoridis and K. Koutroumbas, *Pattern Recognition*, 3rd Ed., Academic Press, San Diego, 2006, pp. 353-362.

[16] Y. Uesaka, "A new Fourier descriptor applicable to open curves," *Trans. IEICE,* vol. 67, no. 8, pp. 166-173, 1984.

[17] N. B. J. Weyland and R. Prasad, "Characterization of line drawings using generalized Fourier descriptors," *Electronics Letters*, vol. 26, no. 21, pp. 1794-1795, 1990.

[18] W. T. Wong, F. Y. Shih, and J. Liu, "Shape-based image retrieval using support vector machines, Fourier descriptors and self-organizing maps," *Information Sciences*, vol. 177, pp. 1878-1891, 2007.

[19] C. T. Zahn and R. Z. Roskies, "Fourier descriptors for plane closed curves," *IEEE Trans. Computers*, vol. 21, no. 3, pp. 269-281, 1972.

[20] D. S. Zhang and G. Lu, "Content-based shape retrieval using different shape descriptors: a comparative study," *Proc. of IEEE ICME*, pp. 317–320, 2001.

[21] D. S. Zhang and G. J. Lu, "A comparative study of Fourier descriptors for shape representation and retrieval," *Proc. ACCV*, pp. 646-651, 2002.

[22] D. S. Zhang and G. J. Lu, "Shape-based image retrieval using generic Fourier descriptor," *Signal Processing: Image Communication*, vol. 17, pp. 825-848, 2002.

Original	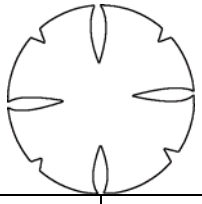	
CR	3%	7%
Conventional [4]	*L*1 = 2.36 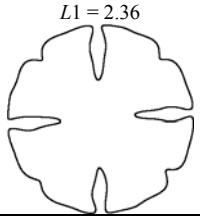	*L*1 = 0.57 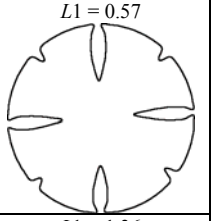
***Seg-FD* +** Uesaka's [16]	*L*1 = 3.27 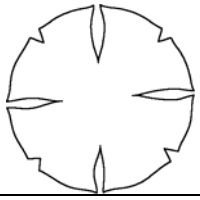	*L*1 = 1.36 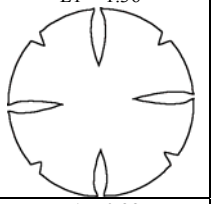
***Seg-FD* +** **Proposed scheme**	*L*1 = 0.57 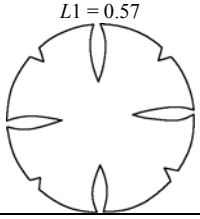	*L*1 = 0.22 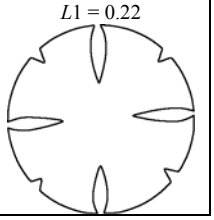

(a)

Original		
CR	3%	7%
Conventional [4]	*L*1 = 3.94 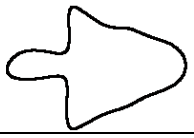	*L*1 = 1.20 
***Seg-FD* +** Uesaka's [16]	*L*1 = 1.27 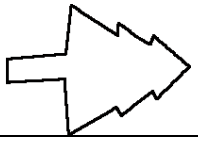	*L*1 = 0.94 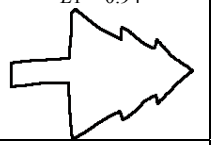
***Seg-FD* +** **Proposed scheme**	*L*1 = 1.26 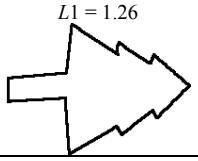	*L*1 = 0.60 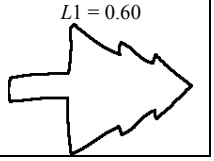

(b)

Fig. 18. Samples of the reconstructed closed boundaries (from the MPEG-7 database) at *CR* = 3% and 7%. The normalized *L*1 distance is also presented. As shown, *Seg-FD* + the proposed Fourier descriptor scheme outperforms the other methods on both the reconstruction quality and the *L*1 error.

Original		
CR	5%	8%
Conventional [4]	*L*1 = 2.24 	*L*1 = 0.79 
***Seg-FD* +** Uesaka's [16]	*L*1 = 1.98 	*L*1 = 1.41 
***Seg-FD* +** **Proposed scheme**	*L*1 = 0.98 	*L*1 = 0.53 

(a)

Original		
CR	5%	8%
Conventional [4]	*L*1 = 2.25 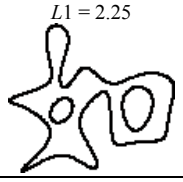	*L*1 = 0.96 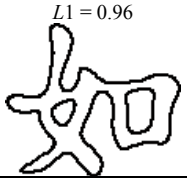
***Seg-FD* +** Uesaka's [16]	*L*1 = 1.32 	*L*1 = 1.03 
***Seg-FD* +** **Proposed scheme**	*L*1 = 1.30 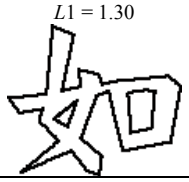	*L*1 = 0.83 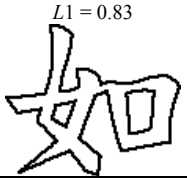

(b)

Fig. 19. Samples of the reconstructed Chinese characters at *CR* = 5% and 8%. The normalized *L*1 distance is also presented. As shown, *Seg-FD* + the proposed Fourier descriptor scheme outperforms the other methods on both the reconstruction quality and the *L*1 error.